

Localization length exponent in two models of quantum Hall plateau transitions

Qiong Zhu,^{1,2} Peng Wu,² R. N. Bhatt,³ and Xin Wan^{2,4}

¹International Center for Quantum Materials, Peking University, Beijing 100871, China

²Zhejiang Institute of Modern Physics, Zhejiang University, Hangzhou 310027, China

³Department of Electrical Engineering, Princeton University, Princeton, New Jersey 08544, USA

⁴Collaborative Innovation Center of Advanced Microstructures, Nanjing 210093, China

(Dated: December 4, 2018)

Motivated by the recent numerical studies on the Chalker-Coddington network model that found a larger-than-expected critical exponent of the localization length characterizing the integer quantum Hall plateau transitions, we revisited the exponent calculation in the continuum model and in the lattice model, both projected to the lowest Landau level or subband. Combining scaling results with or without the corrections of an irrelevant length scale, we obtain $\nu = 2.48 \pm 0.02$, which is larger but still consistent with the earlier results in the two models, unlike what was found recently in the network model. The scaling of the total number of conducting states, as determined by the Chern number calculation, is accompanied by an effective irrelevant length scale exponent $y = 4.3$ in the lattice model, indicating that the irrelevant perturbations are insignificant in the topology number calculation.

I. INTRODUCTION

In the presence of a strong perpendicular magnetic field, the Hall conductance of two-dimensional electron gases at low temperatures is quantized to integral multiples of e^2/h .¹ Tuning either magnetic field or Fermi energy E_f , one can drive an integer quantum Hall transition from one plateau to another. The transition is controlled by a correlation length ξ , which diverges as

$$\xi(E) \sim |E - E_c|^{-\nu}, \quad (1)$$

as the Fermi energy crosses a critical energy E_c (or the magnetic field H crosses a critical value H_c , in which case H replaces E in the above formula). The critical exponent ν is believed to be universal and has been studied extensively both theoretically and experimentally.

Prior to 2009, for non-interacting electrons, the consensus²⁻⁸ was $\nu \approx 2.38 \pm 0.05$. This value was also supported by experiments on samples with short-range scatterers,^{9,10} even though electron-electron interactions are present in experiments, and may be relevant.

Quite unexpectedly, when Slevin and Ohtsuki¹¹ redid the finite-size scaling study of the Chalker-Coddington Network (CCN) model including corrections due to an irrelevant operator, they found $\nu = 2.593 [2.587, 2.598]$, significantly larger than the previously reported values. They found the irrelevant length scale exponent $y \approx 0.17$, which gave rise to large corrections, and altered the exponent ν significantly. Several calculations followed. Obuse et al.¹² reported $\nu = 2.55 \pm 0.01$ and a larger irrelevant length exponent $y = 1.29$. Amado et al.¹³ obtained $\nu = 2.616 \pm 0.014$ but found logarithmic irrelevant length scale correction. Other calculations by Dahlhaus et al.¹⁴, Fulga et al.¹⁵, and Slevin and Ohtsuki¹⁶ in the CCN model also confirmed $\nu = 2.56 \sim 2.6$. Obuse, Gruzberg, and Evers¹⁷ perform a stability analysis of the finite-size scaling of the CCN model and reported $\nu = 2.62 \pm 0.06$, with an irrelevant length scale correction exponent $y \geq 0.4$, which, as the authors pointed out, is considerably larger than most recently reported values. All these works show that with irrelevant length scale correction included, the localization length

exponent $\nu = 2.55 \sim 2.62$. However, the smallness of the leading irrelevant length exponent indicates that great care is needed in numerical studies using finite-size scaling.

Despite the flurry of new and seemingly consistent results, the correct value of the localization length exponent remains under debate. Gruzberg et al.¹⁸ questioned the regular lattice setup of the CCN and considered a general network with geometric disorder. Numerical simulations of this new model found $\nu = 2.374 \pm 0.018$,¹⁸ in agreement with the earlier results. Bondesan et al.¹⁹ developed an effective Gaussian free field approach of the CCN model of the integer quantum Hall plateau transition. Even though the theory confirmed that the spectrum of multifractal dimensions at the transition is parabolic, the authors warned that numerical calculations may suffer from existence of an irrelevant perturbation which is close to marginal (or even marginal).

Consequently, numerical calculations of ν in alternative models^{3,4,20-24} are desirable to help resolve the disagreements, especially ones that are purely two-dimensional, and do not have to rely on the crossover to one-dimension to analyze the data. Earlier, Huo and Bhatt⁴ obtained $\nu = 2.4 \pm 0.1$ in a two-dimensional approach using Chern number calculations in the continuum Landau-level model.⁴ The same result was also found in the disordered Hofstadter model.²²⁻²⁴ No attempt, however, has been made for the two models including corrections due to irrelevant length scales, as done in the CCN model.

In this paper, we revisit the continuum Landau-level model and the Hofstadter lattice model with short-range impurities. After projecting the disorder potential into the lowest Landau level (subband), we calculate the Chern number for all eigenstates to identify the conducting states and perform finite-size scaling of their total number. Combining results in the two models, we obtain a larger exponent $\nu = 2.48 \pm 0.02$ than earlier results $\nu = 2.4 \pm 0.1$, but the two are still consistent, given the larger error bars of the previous work. In addition, we find that the corrections to scaling are very small, (e.g., the irrelevant length exponent is *large*, $y = 4.3 \pm 0.2$ in the lattice model), which can explain the relative accuracy of the earlier results on smaller sizes using the Chern number approach, un-

like transfer matrix methods. We also perform finite-size scaling of the width of the density of conducting states, where the results appear to be less reliable. We attribute this to the fluctuations in the tails of the density of conducting states in finite-sized samples, which renders calculations of higher moments less reliable. Thus, the zeroth moment (the total number of conducting states) is more reliable than the width of density of conducting states, which is the second moment.

The paper is organized as follows. In Sec. II we introduce the two models we study. We briefly review the Chern number calculation method and discuss our scheme for analyzing our data. The next section describes our main results. We first analyze the finite-size scaling of the total number of conducting states in the lattice model and in the continuum model in Sec. III A. Then, we present the finite-size scaling of the width of the density of conducting states in the two models in Sec. III B. We discuss the potential errors in the Chern number calculations in Sec. III C. We summarize our results and discuss our conclusions in light of other work in Sec. IV. In Appendix A we supplement our discussions with additional results in the lattice model, which, in the limit of small magnetic flux per plaquette, evolves smoothly into the continuum model.

II. MODELS AND METHOD

In this paper we present two microscopic models for quantum Hall plateau transitions. The first model describes electrons hopping on a tight-binding lattice with uniform magnetic flux and on-site disorder. The second model describes electrons in continuum with a short-range impurity potential projected into the lowest Landau level. In this section we review the basics of the two models. We also describe the Chern number calculation method used to extract the localization length critical exponent, and the statistical measures used to categorize the data.

A. The lattice model

We consider the two-dimensional tight-binding model

$$\mathcal{H} = - \sum_{\langle i,j \rangle} \left(t e^{i\theta_{ij}} c_i^\dagger c_j + h.c. \right) + \sum_i \epsilon_i c_i^\dagger c_i, \quad (2)$$

where t is the hopping strength and we have $\theta_{ij} = \frac{e}{\hbar} \int_i^j \mathbf{A} \cdot d\mathbf{l}$ in the presence of a perpendicular magnetic field B . We choose the Landau gauge $\vec{A} = (0, Bx, 0)$. The magnetic flux ϕ per unit cell is

$$\frac{\phi}{\phi_0} = \frac{Ba^2}{hc/e} = \frac{1}{2\pi} \sum_{\square} \theta_{ij}, \quad (3)$$

where $\phi_0 = hc/e$ is the flux quantum, and the disorder potentials ϵ_i are independent variables with identical uniform distribution on $[-W, W]$. As the flux ϕ per unit cell varies, the clean model has a self-similar energy spectrum, known as the

Hofstadter butterfly. We choose the flux ϕ per unit cell as $\phi_0/3$. The clean Hamiltonian is translationally invariant and can be diagonalized to three subbands,

$$H_0(\mathbf{k})|\phi_n(\mathbf{k})\rangle = E_n(\mathbf{k})|\phi_n(\mathbf{k})\rangle, \quad (4)$$

where the subband index $n = 0, 1, 2$. The three subbands carry Chern number 1, -2, and 1, and each contains $N_\phi = L_1 L_2 / 3$ states for an $L_1 \times L_2$ lattice. In the full model the evolution of the conducting states in the lowest subband is correlated with the central band and may introduce additional complexity.²² Therefore, we truncate the Hilbert space by projecting the disorder potentials into the lowest subband,

$$\tilde{V} = \sum_{\mathbf{k}, \mathbf{k}'} |\phi_0(\mathbf{k})\rangle \langle \phi_0(\mathbf{k})| V(\mathbf{r}) |\phi_0(\mathbf{k}')\rangle \langle \phi_0(\mathbf{k}')|. \quad (5)$$

Earlier work of Thouless conductance found that the critical behavior is independent of the ratio t/W when $t/W \leq 0.2$.²⁴ Hence, we set $t = 0$ and $W = 1$ after the projection. In this case the clean band width is reduced to zero so we have particle-hole symmetry; this fixes the critical energy at $E_c = 0$.

B. The continuum model

We consider the two-dimensional electron in presence of a magnetic field

$$H = \frac{1}{2m} (\mathbf{P} + \frac{e}{c} \mathbf{A})^2 + V(\mathbf{r}) = \frac{\Pi^2}{2} + V(\mathbf{r}), \quad (6)$$

where the symmetric gauge $\mathbf{A} = \frac{1}{2}B(y, -x)$ is used, and $V(\mathbf{r})$ is the random potential. The generator of infinitesimal magnetic translation is

$$\kappa \equiv (\kappa_1, \kappa_2) = \mathbf{P} - \frac{e}{c} \mathbf{A} = \Pi(-B), \quad (7)$$

with $[\kappa_1, \kappa_2] = -i$, where we set the magnetic length $l_B = 1$ and $\hbar = 1$ for convenience. For a finite $L_1 \times L_2$ system, the translation operator $t(L_j \hat{e}_j) = \exp(i\kappa_j L_j)$ satisfies the magnetic algebra

$$t(\mathbf{a})t(\mathbf{b}) = \exp[i(\mathbf{a} \times \mathbf{b}) \cdot \hat{z}] t(\mathbf{b})t(\mathbf{a}). \quad (8)$$

When the number of flux quanta in an $L_1 \times L_2$ sample $N_\phi = L_1 L_2 / (2\pi)$ is an integer, $t(L_1 \hat{e}_1)$ and $t(L_2 \hat{e}_2)$ commute with each other. By defining two primitive translations, $t_j = t(L_j / N_\phi \hat{e}_j) = \exp(i\kappa_j L_j / N_\phi)$ for $j = 1, 2$, we are able to construct a Landau-like stripe basis $|\phi_m\rangle$ in the lowest Landau level by requiring

$$\begin{cases} t_1 |\phi_m\rangle = |\phi_{m+1}\rangle, \\ t_2 |\phi_m\rangle = \exp(-i2\pi m / N_\phi) |\phi_m\rangle. \end{cases} \quad (9)$$

We consider randomly placed scatterers with δ -potential, i.e. $V(\mathbf{r}) = \sum_i^{N_{\text{imp}}} \delta(\mathbf{r} - \mathbf{r}_i)$, whose Fourier components are $V_{\mathbf{q}}$. The number of short-range scatterers is chosen to be $16N_\phi$.

The random potential is then projected into the lowest Landau level

$$\tilde{V} = \sum_{j,k} |\phi_j\rangle\langle\phi_j| \sum_{\mathbf{q}} V_{\mathbf{q}} e^{i\mathbf{q}\cdot\mathbf{r}} |\phi_k\rangle\langle\phi_k|, \quad (10)$$

where $\mathbf{q} = (q_1, q_2) = (2\pi m/L_1, 2\pi n/L_2)$ and m, n are integers.

For simplicity, we consider square samples $L_1 = L_2 = L$ with generalized boundary condition

$$t(L\hat{e}_j)|\psi\rangle = e^{i\theta_j}|\psi\rangle, \quad j = 1, 2, \quad (11)$$

with $\theta_j \in [0, 2\pi]$, the Hamiltonian matrix is calculated as

$$H_{jk}(\theta_1, \theta_2) = \sum_{m,n} V_{mn} e^{-\pi(m^2+n^2)/2N_\phi} e^{-i\pi mn/N_\phi} \times e^{i[m\theta_2-n\theta_1]/N_\phi} e^{-i2\pi mj/N_\phi} \langle\phi_j|\phi_{k-n}\rangle. \quad (12)$$

For particle-hole symmetric potential, the critical energy is also expected at $E_c = 0$.

C. The Chern number calculation

In either case, we can impose generalized boundary conditions. The boundary condition averaged Hall conductance for a state ψ_m is a topological invariant²⁶

$$\langle\sigma_{xy}(m)\rangle = C(m) \frac{e^2}{h}, \quad (13)$$

where the first Chern number

$$C(m) = \frac{1}{2\pi i} \int_0^{2\pi} \int_0^{2\pi} d\theta_x d\theta_y \left[\left\langle \frac{\partial\psi_m}{\partial\theta_x} \middle| \frac{\partial\psi_m}{\partial\theta_y} \right\rangle - h.c. \right]. \quad (14)$$

For efficient numerical calculation, we follow the method of Fukui et al.²⁷ We divide the $2\pi \times 2\pi$ boundary condition space into a grid of $L_g \times L_g$ sites

$$\vec{\theta} = (\theta_x, \theta_y) = \frac{2\pi}{L_g} (l_x, l_y), \quad l_x, l_y = 0, \dots, L_g - 1, \quad (15)$$

so primitive vectors $\hat{\mu}$ are vectors in the directions of $\mu = x$ and y with length $2\pi/L_g$. For the m th eigenstate, we define a $U(1)$ link variable

$$U_\mu^m(\vec{\theta}) = \langle\phi_m(\vec{\theta})|\phi_m(\vec{\theta} + \hat{\mu})\rangle / N_\mu^m(\vec{\theta}), \quad (16)$$

where $N_\mu^m(\vec{\theta}) = |\langle\phi_m(\vec{\theta})|\phi_m(\vec{\theta} + \hat{\mu})\rangle|$ is the normalization factor. The Berry phase in a unit cell at $\vec{\theta}$ is then calculated by a gauge invariant formula

$$\gamma_m(\vec{\theta}) = \frac{1}{i} \ln U_x^m(\vec{\theta}) U_y^m(\vec{\theta} + \hat{x}) U_x^m(\vec{\theta} + \hat{y})^{-1} U_y^m(\vec{\theta})^{-1}.$$

For a sufficiently fine grid, the local Berry phase is small in amplitude and can be restricted to $(-\pi, \pi]$ in numerical calculation. The Chern number $C(m)$ is obtained by summing the phase over all lattice sites

$$C(m) = \frac{1}{2\pi} \sum_{\vec{\theta}} \gamma_m(\vec{\theta}). \quad (17)$$

Due to the introduction of the locally gauge-invariant formulation of Chern number, the efficiency of the method has been improved greatly even with a coarsely discretized boundary condition space. As pointed by Arovas et al.,²⁸ the sensitivity of the nodes of the wave function to the smooth change in boundary conditions can be used to distinguish the localized and extended states. Consequently, we follow Huo and Bhatt⁴ to identify states with nonzero Chern numbers as conducting states.

The total number of conducting states per sample is defined as

$$N_c = \int_{-\infty}^{\infty} \rho_c(E) dE, \quad (18)$$

where $\rho_c(E)$ is the density of conducting states. In the vicinity of the critical energy E_c , the localization length diverges as $\xi(E) \sim |E - E_c|^{-\nu}$. For a finite size system with linear size $L \sim \sqrt{N_\phi}$, one expects that the states with $\xi(E) > L$ are conducting. The number of such states scale as $N_c \sim L^2 \rho(E_c) |E_m - E_c| \sim N_\phi^{1-1/(2\nu)}$, to the lowest order, where E_m is determined by $\xi(E_m) \sim L$. One can also define the width of $\rho_c(E)$ as the square root of its second moment

$$\Delta E = \left[\frac{\int_{-\infty}^{\infty} (E - E_c)^2 \rho_c(E) dE}{\int_{-\infty}^{\infty} \rho_c(E) dE} \right]. \quad (19)$$

Roughly speaking, the width is set by $L \sim \xi(E) \sim \Delta E^{-\nu}$, so it is expected to follow $\Delta E \sim L^{-1/\nu} \sim N_\phi^{-1/(2\nu)}$. The lowest-order scaling of N_c and ΔE may need irrelevant length corrections.

D. Goodness of fit

In this paper we compare various scaling hypotheses with and without irrelevant length corrections. After obtaining the best-fit values of parameters, we need to decide which hypothesis is the best description of the data. Our result of the critical exponent is then obtained from the best-fit with the best hypothesis. In this subsection, we discuss the acceptability of the scaling hypothesis.

Generally speaking, we fit N data points (x_n, y_n) with $n = 0, \dots, N-1$ with measurement errors σ_n to a model that has M adjustable parameters a_0, \dots, a_{M-1} . The model has a functional relationship between the measured variables and parameters $y(x) = y(x; a_0, \dots, a_{M-1})$, minimizing the parameters a_0, \dots, a_{M-1} is equivalent to minimizing the chi-square

$$\chi^2 \equiv \sum_{n=0}^{N-1} \left[\frac{y_n - y(x_n; a_0, \dots, a_{M-1})}{\sigma_n} \right]^2. \quad (20)$$

A typical value of χ^2 for a moderately good fit is $\chi^2 \approx \text{dof}$, where $\text{dof} = N - M$ is the degrees of freedom, or, equivalently, the reduced chi-square $\bar{\chi}^2 \equiv \chi^2/\text{dof} \approx 1$. Relatively smaller value of χ^2 indicates a better fit. However, one must

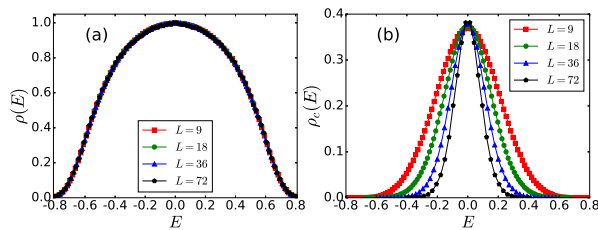


FIG. 1. (a) Disorder averaged total density of states $\rho(E)$ and (b) density of conducting states $\rho_c(E)$ in the lattice model for system sizes $L = 9, 18, 36,$ and 72 .

also take into account the number of adjustable parameters used in the fit, to determine the overall acceptability of the fit. A quantitative measure of the goodness-of-fit is given by the cumulative probability function $Q(\chi^2|\text{dof})$, which is the probability that the observed chi-square will exceed a particular values χ^2 by chance even for a correct model²⁹

$$Q(\chi^2|\text{dof}) = 1 - P\left(\frac{\text{dof}}{2}, \frac{\chi^2}{2}\right), \quad (21)$$

where $P(a, x)$ is the incomplete Gamma function. A larger value of Q is taken as an indicator of a better fit. If Q is too small, the reason could be either the model is unlikely to be true and can be rejected, or the size of the measurement errors σ_n are larger than stated. If Q is close to 1, it could be caused by overestimation of the measurement errors.

III. RESULTS

A. The number of conducting states

We begin with the study of square lattices with $L = 6$ -81. The largest system contains almost 30 times more states than the largest did twenty years ago.²² The number of disorder realizations ranges from 10^5 for $L = 6$ to 10^2 for $L = 81$. In the Chern number calculation we choose a grid size such that the number of grid points along in each dimension is $L_g = 30$ for $L \leq 30$ and $L_g \approx \sqrt{2/3}L$ for $L = 36$ -81. Figure 1 shows the density of states $\rho(E)$ and the density of conducting states $\rho_c(E)$ for several system sizes.

The total density of states $\rho(E)$ remains the same bell shape for all system sizes, while the density of conducting states $\rho_c(E)$ shrinks as the system size increases, implying that in the thermodynamic limit only states with $E = 0$ are extended. To prove this, we follow the same procedure in earlier literature^{4,22} to study the scaling behavior of the total number of conducting states per sample N_c and the width ΔE of the density of conducting states $\rho_c(E)$, which are the zeroth and (the normalized) second moment of the density of nonzero Chern states.

We begin by fitting the number of conducting states to

$$N_c^{\text{power}} = aN_\phi^{1-1/(2\nu)}. \quad (22)$$

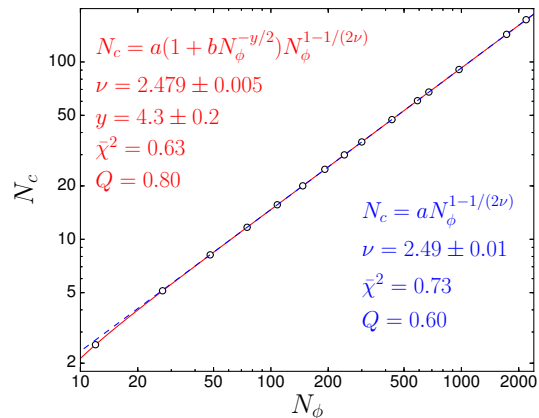


FIG. 2. Log-log plot of the number of conducting states per sample N_c versus the total number of states per sample N_ϕ in the lattice model. The percentage precisions for the data are 0.07% to 0.2% for $L = 6$ to 54, 0.5% for $L = 72$, and 1% for $L = 81$. The blue dashed line is the power-law fit without corrections (a straight line) for $L \geq 30$. The number of data, number of parameters, chi-squared, and goodness of fit are 7, 2, 3.66, and 0.60, respectively. The solid red line shows the fit with irrelevant length corrections for all the data. The number of data, number of parameters, chi-squared, and goodness of fit are 15, 4, 6.94, and 0.80, respectively.

A chi-square fitting yields $\nu = 2.49 \pm 0.01$, as shown by the blue dashed line in Fig. 2. The reduced chi-square $\bar{\chi}^2 = 0.732$ and the goodness of fit $Q = 0.599$. The straightforward power-law fit for all system sizes results in a good description of the data. Deviation is visually noticeable only for $L = 6$ in Fig. 2. This can be improved if we include the irrelevant length scale corrections.

The leading correction can be accounted for by assuming

$$N_c^{\text{irr}} = a(1 + bN_\phi^{-y/2})N_\phi^{1-1/(2\nu)}, \quad (23)$$

where y is the leading irrelevant length exponent. A chi-square fitting now yields $\nu = 2.479 \pm 0.005$ and $y = 4.3 \pm 0.2$, as illustrated in Fig. 2. The reduced chi-square $\bar{\chi}^2 = 0.631$ and the goodness of fit $Q = 0.804$. One expects this form is valid only for $|bN_\phi^{-y/2}| \ll 1$. Indeed, the correction term $bN_\phi^{-y/2}$ varies from -0.06 for $L = 6$ to -10^{-7} for $L = 81$. With or without the correction, the critical exponent ν remains unchanged within error bars. This is supported by the similar $\bar{\chi}^2$ or Q for the two fits. The inclusion of the irrelevant perturbation, in principle, fits the data better with the larger number of parameters. However, it is debatable whether the improvement is enough to warrant increasing the number of parameters. It is worth pointing out that the best fit to the irrelevant length exponent is large, $y = 4.3$. This is strong evidence that the irrelevant (or marginal) perturbation at the criticality has a weak effect on the Chern number calculation and the scaling of the number of conducting states.

For the continuum model, we study system size from $N_\phi = 16$ to 3,072, with disorder realizations from 40,000 for $N_\phi = 16$ to 608 for $N_\phi = 3,072$. In the Chern number calculation

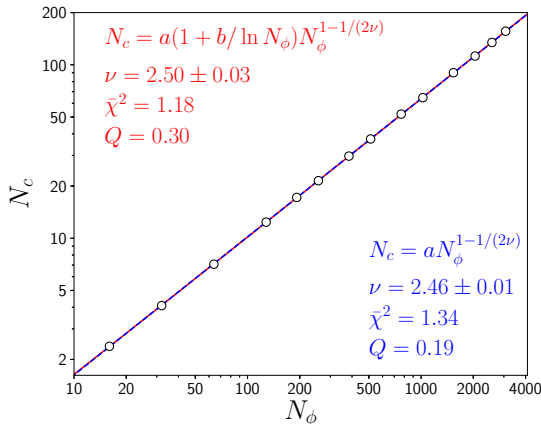


FIG. 3. Log-log plot of the number of conducting states N_c vs. N_ϕ in the continuum model. The percentage precisions of the data are 0.31% to 0.48% for $N_\phi = 16$ to 3,072. The blue dashed line is the power-law fit without any corrections. The number of data, number of parameters, chi-squared, and goodness of fit are 14, 2, 16.10, and 0.19, respectively. The red solid line shows the fit with logarithmic corrections. The number of data, number of parameters, chi-squared, and goodness of fit are 11, 3, 12.93, and 0.30, respectively.

we use grid size $L_g = 50$ for all system sizes. Fig. 3 fits the number of conducting states as $N_c = aN_\phi^{1-1/(2\nu)}$. For all available 14 system sizes, we find $\nu = 2.46 \pm 0.01$ with $\bar{\chi}^2 = 1.34$ and $Q = 0.19$. We emphasize that there are no irrelevant length corrections in the fitting, and the exponent is in good agreement with the value obtained above in the lattice model. We also fit data only in systems with $N_\phi \geq 256$, the result is $\nu = 2.46 \pm 0.02$ with $\bar{\chi}^2 = 0.67$ and $Q = 0.70$. The exponent agrees with the previous one for all systems, but the error bar is now larger due to the fewer system sizes.

The agreement in ν between all systems and larger system only already suggests that the existence of the irrelevant length corrections in the continuum model is difficult to demonstrate. Attempt to fit all data with the corrections leads to large error bars in $\nu = 2.47 \pm 0.01$ and $y = 8.7 \pm 23.6$, which indicates that a single leading irrelevant length correction is not a good hypothesis. It is possible that the existence of a dangerous (or marginal) irrelevant operator may cause slower disappearing corrections to scaling. We attempt to fit all data in the continuum model to a power law with logarithmic corrections

$$N_c^{\text{log}} = a(1 + c/\ln N_\phi)N_\phi^{1-1/(2\nu)}. \quad (24)$$

As illustrated in Fig. 3, it yields $\nu = 2.50 \pm 0.03$ with $\bar{\chi}^2 = 1.18$ and $Q = 0.30$. With the logarithmic corrections, the reduced chi-square is now smaller while the goodness of fit is larger. The resulting exponent $\nu = 2.50$ is larger but agrees, within the error bars, with the value in the absence of the corrections.

We can compare the differences between the fit without corrections [Eq. (22)] and the one with logarithmic corrections [Eq. (24)] by plotting the ratio of the two, as well as the properly scaled raw data, as shown in Fig. 4. In the figure

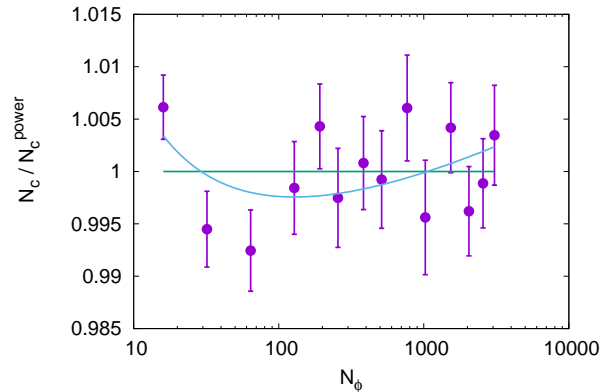


FIG. 4. Rescaled plot of Fig. 3 of the power-law fits of the total number of conducting states without irrelevant length corrections (the horizontal line) and that with logarithmic corrections (the curved line). To visualize the errors of the data from very different sizes, we rescaled all data and fits by the power-law fit without corrections.

the horizontal line at 1 represents the power-law fit N_c^{power} . The scattered data points, scaled by $1/N_c^{\text{power}}$, are all within 2σ , or twice the corresponding error bars. The fit with log corrections N_c^{log} , scaled by $1/N_c^{\text{power}}$, curves up, fitting the data from the three smallest systems better than the horizontal line. Unless it is necessary to consider the systems as small as $N_\phi = 16$ or 32, the power-law fit without corrections is essentially as good as the one with logarithmic corrections. But if so, it remains very interesting to understand why the topological number calculation can support excellent scaling for more than one order of magnitude in linear scale starting from such small systems. Based on the comparison, if the trend of data persists (including error bars), we would only be able to distinguish the two if we could approach $N_\phi > 40,000$.

Combining the results of the different fits in both the lattice model and the continuum model, we conclude that the scaling of the total number of conducting states yields a consistent value $\nu = 2.48 \pm 0.02$.

B. The width of the density of conducting states

While the critical exponent ν is found to be universal in different models as well as using different measures, as expected, our fits including one irrelevant (or marginal) correction term yields different results for the irrelevant length exponent from different quantities. To show this, we consider the width ΔE of the density of conducting states. With the corrections of the leading irrelevant length, one expects $\Delta E = c(1 + dN_\phi^{-y/2})N_\phi^{-1/(2\nu)}$. A chi-square fitting gives $\nu = 2.40 \pm 0.02$ and $y = 1.2 \pm 0.1$ with the reduced chi-square $\bar{\chi}^2 = 1.032$ and the goodness of fit $Q = 0.415$, as shown in Fig. 5. The correction term $dN_\phi^{-y/2}$ varies from -0.12 for $L = 6$ to -0.005 for $L = 81$. The correction is twice as large for small system sizes as that in the scaling of N_c , which suggests that we may need to consider additional corrections;

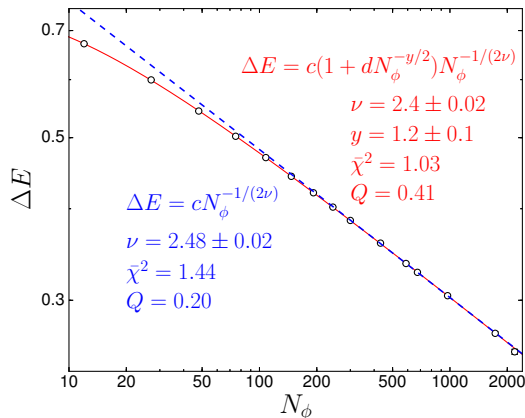


FIG. 5. Log-log plot of the width ΔE of the density of conducting states vs. N_ϕ in the lattice model. The percentage precisions of the data are 0.06% to 0.17% for $L = 6$ to 54, 0.44% for $L = 72$, and 0.78% for $L = 81$. The red solid line shows the power-law fit with leading irrelevant length corrections for all data points. The number of data, number of parameters, chi-squared, and goodness of fit are 15, 4, 11.35, and 0.41, respectively. The blue dashed line is the power-law fit without any corrections for systems with $L \geq 30$ (or $N_\phi \geq 300$). The number of data, number of parameters, chi-squared, and goodness of fit are 7, 2, 7.22, and 0.20, respectively.

such a fit may result in a different value of y .

The comparison of the scalings of N_c and ΔE shows that even with the same set of data, namely $\rho_c(E)$, one obtains exponent ν with a slight difference. Judging from the smaller size of the corrections and, in particular, the larger value of y , we conclude that the scaling of N_c is more reliable. This is consistent with empirical evidence from simulations of other disordered systems such as spin glasses that lower order moments of distributions can be calculated more reliably (they also seem to converge faster to equilibrium than high order moments). An additional evidence is that we can perform a power-law fitting of ΔE without the irrelevant length corrections, $\Delta E \sim cN_\phi^{-1/(2\nu)}$, for system sizes $L \geq 30$ (i.e., $N_\phi \geq 300$), as shown by the blue dashed line in Fig. 5. The result is $\nu = 2.48 \pm 0.02$ with $\bar{\chi}^2 = 1.444$ and $Q = 0.205$. Therefore, the value obtained from larger systems is consistent with that obtained from the scaling of N_c .

The comparison suggests that the tails of the density of conducting states $\rho_c(E)$ suffer more from the finite-size effects. The width ΔE is related to the second moment of $\rho_c(E)$, while N_c is the zeroth moment of $\rho_c(E)$. Therefore, ΔE amplifies the finite-size fluctuations in the tails, or at energies far from the critical energy. If this understanding is correct, we could expect that in a different model but with the same method the scaling of N_c would generate the consistent universal ν , even though corrections to scaling could be different. However, the scaling of ΔE using finite sizes could give a different ν , whose value depends on the non-universal finite-size fluctuations in the tails.

An independent confirmation of the tail effect comes from the study of the perturbations to the disordered potential. We

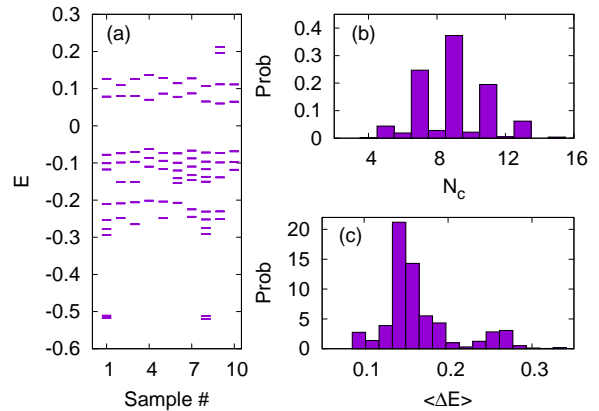


FIG. 6. (a) Energies of the conducting states in 10 samples ($L = 12$ or $N_\phi = 48$), whose on-site potentials differ only by 5% fluctuations. Pairs of conducting states can emerge far from the band center. (b) Distribution of the number of conducting states in each sample from 1,000 realizations. With the constraint that the total Chern number per sample is +1, the distribution shows strong odd-even difference, but is bell-shaped either for odd N_c or for even N_c . (c) The root-mean-square energy for conducting states in each sample for the same 1,000 realizations. The distribution has a long tail with additional peaks.

start with an arbitrary disorder realization in a 12×12 lattice and perturb it with an additional disordered potential, whose strength is 5% of the original one. The additional potential distorts the energy spectrum and likely causes a pair of energy levels to cross each other. As a result, the Chern number of the pair can change. Since most states are localized, the change creates a pair of conducting states with Chern numbers +1 and -1, as demonstrated in Fig. 6(a). The pair, if lying in the tail, can affect the width of the conducting states much more significantly than their total number. For illustration, we analyze 1,000 samples which differ from each other only by the 5% fluctuations. Figure 6(b) plots the distribution of the number of conducting states N_c in each sample. N_c vary from 4 to 15 with strong odd-even fluctuations, because the total Chern number in each sample is constrained to be +1 and most conducting states carry Chern number +1 or -1. Other than the odd-even effect, the distribution is bell-shaped with a well defined peak at $N_c = 9$. We expect that the total number is self-averaged in the thermodynamic limit and hence well-behaved. On the other hand, Fig. 6(c) plots the distribution of the root-mean-square energy of the conducting states in each sample for the same 1,000 realizations. The distribution is clearly not bell-shaped. Well above the main peak at 0.14, we can find a significant bump around 0.26 and the tail extends to as large as 0.33. The multiple-peak structure is consistent with the emergence of conducting pairs far from the center, as shown in Fig. 6(a). But such pairs do not cause the distribution of N_c to deviate significantly from the bell shape. Therefore, We lean toward the scaling results of N_c , rather of ΔE , based on the study of the fluctuations.

We study the scaling of the width ΔE of the density of conducting states $\rho_c(E)$ in the continuum model next. If we fit

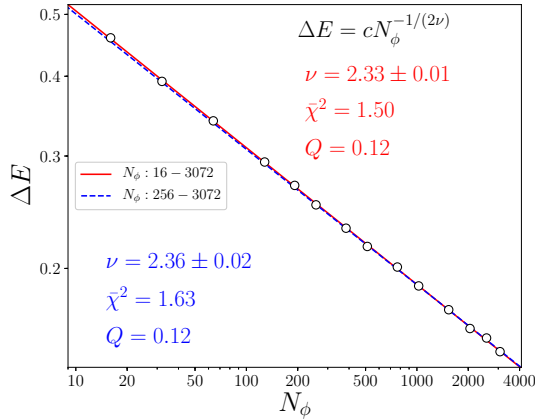


FIG. 7. Log-log plot of the width ΔE of the density of conducting states vs. N_ϕ in the continuum model. The percentage precisions of the data vary between 0.31% and 0.45% for $N_\phi = 16$ to 3,072. The red solid line is the power-law fit for the data points from $N_\phi = 16$ to $N_\phi = 3,072$. The number of data, number of parameters, chi-squared, and goodness of fit are 14, 2, 18.0, and 0.12, respectively. The blue dashed line is the fit for the data points from $N_\phi = 256$ to $N_\phi = 2048$. The number of data, number of parameters, chi-squared, and goodness of fit are 9, 2, 11.4, and 0.12, respectively.

all data to the form $\Delta E = cN_\phi^{-1/(2\nu)}$, we obtain $\nu = 2.33 \pm 0.01$ with the reduced chi-square $\bar{\chi}^2 = 1.50$ and the goodness of fit $Q = 0.12$. When we only fit data with $N_\phi \geq 256$, we obtain $\nu = 2.36 \pm 0.02$ with $\bar{\chi}^2 = 1.63$ and $Q = 0.12$. Within the error bars, we cannot draw a definite conclusion on the trend of ν in the thermodynamic limit. Like the scaling of N_c , including either power-law corrections or logarithmic corrections shows no significant improvement.

As we discussed at the end of Sec. III A, the localization length critical exponent ν obtained from the scaling of N_c is consistent in the lattice model and the continuum model. However, the values of ν obtained from the scaling of ΔE in the two models are not. The observations confirm that the finite-size fluctuations are more significant in the tails of the density of conducting states. In other words, the values obtained from the scaling of ΔE are less reliable, unless we can approach much larger system sizes. We also studied the width of the density of conducting states for different percentiles and found that the fluctuations are too large to allow accurate analysis.

C. Errors in the Chern Number calculation

Because Chern number, or the dimensionless Hall conductance, is a topological invariant, the main errors in the Chern number approach come from the discretization of the boundary condition space into a grid. The accuracy of Chern numbers thus depends on the grid size L_g . But increasing L_g will slow down the Chern number calculation. To estimate the optimal L_g , e.g., in the lattice model, we consider uniformly distributed γ_m in Eq. (17) in the boundary condition space. For

a state m with Chern number $C(m)$, we expect

$$\bar{\gamma}_m = \frac{2\pi C(m)}{L_g^2}, \quad (25)$$

for each $\vec{\theta}$. Sign errors of γ_m occur due to the restriction of the phase to $(-\pi, \pi]$ when γ_m is comparable to π , i.e.,

$$\frac{2\pi C(m)}{L_g^2} \sim \epsilon\pi \quad (26)$$

where ϵ can be understood as the error rate of the state. This gives a rough estimate of the error rate per state with $C(m) = O(1)$ as $\epsilon \sim 2/L_g^2$.

We implement a simple consistency check for the Chern number calculation: the total Chern number of each sample should be one. When we obtain a sample that fails the total Chern number check, we reject all states in the sample. This happens when at least one of the states in the sample has an incorrect Chern number. For small enough ϵ , the rejection rate r for a sample with $L^2/3$ states is

$$r \approx \epsilon (L^2/3) \sim \frac{2}{3} \left(\frac{L}{L_g} \right)^2 \quad (27)$$

Therefore, in the lattice model we choose $L_g \approx \sqrt{2/3}L$ for $L \geq 36$ and $L_g = 30$ for $L \leq 30$, in order to keep the rejection rate low.

We also run numerical tests to estimate the error rate of the Chern number calculation for individual states and the consequent errors in N_c and ΔE , which we use to extract ν . In the tests we study the computational errors of lattice systems with linear size $L = 6-21$, each with $N_s = 10,000$ random potential realizations. Our calculation finds that the rejection rate r vanishes as $L_g^{-\eta}$ with η varying between 2.5-3.3, which decreases even faster than our simple expectation. When we fix $L_g = 30$, the rejection rate r is no more than 5×10^{-3} and increases with size as $L^{1.6}$, which is close to L^2 as we expect in Eq. (27). The better-than-expected observations are likely due to the fact that the majority of the Chern numbers is zero and their percentage increases with L . With the numerical results, we can assume that Chern numbers calculated with $L_g = 60$ are sufficiently accurate and can be used as a reference. We then calculate Chern numbers with $L_g = 30$. By comparing them, we estimate the relative error in N_c is around 10^{-3} and the relative error in ΔE is even smaller. Compared to the sample-to-sample fluctuations, we find the errors due to the Chern number calculation are at least one order of magnitude smaller and can be neglected. The measurement errors in the preceding subsections are, therefore, the standard error in the mean of the relevant data.

IV. SUMMARY AND DISCUSSION

In this work, we have conducted a detailed study of two models for the integer quantum Hall plateau transition: the disordered Hofstadter lattice model and the continuum

Landau-level model. We perform high-precision Chern number calculation for system size up to $N_\phi = 2,187$ in the lattice model and 3,072 in the continuum model. We use multiple measures to rule out the errors in the Chern number calculation caused by the discretization of the integration grid. Using nonzero Chern number as criterion, we calculate the density of conducting states $\rho_c(E)$ for various system sizes.

By fitting the total number of conducting states N_c to a power law, we obtain the localization length critical exponent $\nu = 2.49 \pm 0.01$ in the lattice model and $\nu = 2.46 \pm 0.01$ in the continuum model. In the lattice model we obtain $\nu = 2.479 \pm 0.005$ with better goodness of fit after we include the leading irrelevant length corrections. However, the bare power-law fit cannot be improved in the continuum model by the inclusion of the leading irrelevant length corrections. With systems as small as $N_\phi = 16$, a fit with logarithmic corrections, which may be caused by a dangerous (marginal) irrelevant perturbation, yields $\nu = 2.50 \pm 0.03$. Based on these results, we conclude that the two models are in the same universality class and $\nu = 2.48 \pm 0.02$. The larger exponent is found in much larger systems than in the earlier studies. In fact the largest system in the present study has 24 times the flux quanta of that in the earlier study for the continuum model,⁴ and almost 30 times the flux quanta for the previous lattice model.²² However, given the fact that earlier studies had large error bars of 0.1, the new result is still consistent with the earlier estimates.^{4,22,23}

Our analysis of both models, using fully two-dimensional scaling, suggests that corrections to scaling due to irrelevant operators are small, unlike what is found in strip-geometry methods using the crossover to one-dimension to extract critical exponents. Even in the lattice model where the corrections are apparently larger, the leading irrelevant length exponent is found to be $y = 4.3 \pm 0.2$, which is substantially larger than the value found in the methods using the crossover to one dimension using the strip geometry on the CCN model. This suggests that in the topological number based calculation the leading irrelevant correction may have small amplitude. Because of this, the precise value of the best-fit irrelevant length exponent varies depending on the model and presumably therefore has greater uncertainty, though it is certainly large. On the other hand, the smaller corrections to scaling would explain why the earlier Chern number calculations revealed the consistent result of $\nu = 2.4 \pm 0.1$ in systems with no more than 128 magnetic flux quanta.⁴

We also attempt to determine ν from the scaling of the width of the density of conducting states $\rho_c(E)$, which is related to the second moment of ρ_c . The value is found to be appreciably smaller than that obtained by the scaling of N_c and is model-dependent: 2.40 ± 0.02 for the lattice model and 2.33 ± 0.01 for the continuum model. Fitting the data from larger systems only in the lattice model gives $\nu = 2.48 \pm 0.02$, which is then consistent with the value from the scaling of N_c . This suggests that higher moments (e.g. the second moment) of the distribution of the nonzero Chern number states are subject to greater error than the total number (zereth moment). Our further analysis attributes this to the random fluctuations of conducting states in the band tails. Therefore, the agree-

ment of the critical exponent obtained from the total number and the width of the conducting states in the earlier study⁴ are likely due to the large error bars.

The localization length critical exponent $\nu = 2.48 \pm 0.02$ in the present study differs from the value (varying from 2.55 to 2.62) found in recent studies of the CCN model.¹¹⁻¹⁷ One possibility, which requires further work, is the issue of whether the CCN model and the non-interacting quantum Hall transition in a Landau level belong to the same universality class, as was believed for several years. This has recently been challenged by Gruzberg and coworkers,¹⁸ who argued that the CCN model may not capture all types of disorder that are relevant at the integer quantum Hall plateau transition. However, the authors¹⁸ found in the numerical simulation of a geometrically disordered network model $\nu = 2.374 \pm 0.018$, which is significantly smaller than that found in the present study for the lattice model and the continuum model.

Very recently, *after our manuscript was in the referee process*, Puschmann and coworkers³⁰ found a localization length exponent $\nu = 2.58 \pm 0.03$ in strips of microscopic lattices, which is consistent with the CCN model. The lattice model contains all subbands, unlike the one used in the present study, which projects the disordered potential to the lowest subband with Chern number +1. The authors³⁰ employed a scheme based on crossover to one-dimensional systems and showed that the scaling of the Lyapunov exponent depends on flux per plaquette ϕ and converges for $\phi \leq 1/10$. In particular, they found that the corrections to scaling for $\phi = 1/3$ and $1/4$ deviate significantly from the small flux limit, which are expected to be identical to the results of the continuum model. In contrast, we find that in the projected lattice model, in which there are no subband mixings by design, the results for $\phi = 1/3$ is consistent with those in the continuum model, *with or without corrections*, based on purely two-dimensional scaling analysis. We emphasize that in both lattice studies, the scaling behavior persists for well over one order of magnitude in linear size change.

There is yet another possibility for the remaining discrepancies. Zirnbauer³¹ suggested that $1/\nu$ and y can keep decreasing as the renormalization group fixed point is approached. While we find no direct evidences supporting the scenario, this means that the approach to the ultimate scaling behavior can be much slower than we thought. If this is the case, the puzzle on the localization length exponent can only be resolved with much larger system sizes.

V. ACKNOWLEDGEMENTS

The authors thank Ferdinand Evers, Ilya Gruzberg, Tomi Ohtsuki, Martin Puschmann, Keith Slevin, and Thomas Vojta for helpful discussions. This work was supported by the 973 Program under Project No. 2012CB927404, by the NSFC under Grant No. 11174246, and by U.S. DOE-BES Grant DE-SC0002140 (RNB). RNB also thanks the hospitality of the Aspen Center for Physics for a stay during which the manuscript was being finalized.

Appendix A: Universality from the Lattice to the Continuum Model

In the main text we study the lattice model and the continuum model, and our results confirm that the two are in the same universality class, as was expected in earlier studies.⁶ The particular choice of magnetic flux per plaquette we made is $\phi = 1/3$. In the pure case, the band width of the lowest magnetic subband is not small (in units of the hopping strength t), compared with the gap separating the lowest and the central subbands. To avoid band mixing, we project the Hamiltonian to the subspace of the lowest subband. A side advantage is that we deal with a smaller Hilbert space dimension, hence the Chern number calculation is faster. The choice of ϕ is not restricted. In the case of $\phi = 1/i$, where $i > 2$ is an integer, the spectrum of the full Hamiltonian contains i subbands (the central two are touching at $E = 0$ for even i). The lowest (and the highest) subband for every integer i is characterized by Chern number $+1$ and can be used to study the plateau transition. For sufficiently large i , the band width of the lowest subband in the pure case is much smaller than the adjacent band gap, hence the spectral projection is not necessary. In principle, other subbands, with the exception of the central band(s), can model a Landau level as well; but they are known to have longer localization length, which can be overcome by, e.g., a correlated disorder potential.²⁴

In addition to the localization length ξ and the microscopic lattice constant a , we have a third length scale: the magnetic length $l_B = a\sqrt{i/(2\pi)}$. In the limit of large i , a/l_B goes to zero. Therefore, we can regard the continuum model as the limit of large i and expect that the localization length critical exponent extracted in the lattice model with larger i is consistent with the results for $\phi = 1/3$ and in the continuum model. However, *subsequent to the online publication of this work*, a study of the tight-binding lattice model in the absence of the subband projection³⁰ found $\nu = 2.58 \pm 0.03$ for $\phi \geq 1/10$ with pronounced corrections to scaling. The authors there applied the Green's function method on a strip geometry and perform finite-size scaling of the dimensionless Lyapunov exponent by varying the strip width. For $\phi = 1/3, 1/4$, and $1/5$, the authors found non-universal behavior, which they attributed to the non-negligible intrinsic LL width.

In this Appendix, we provide additional data and analysis to show that the critical exponent $\nu = 2.48 \pm 0.02$ in the main text is universal for both the projected lattice model, regardless of i , and the continuum model. In the projected model, the width of the magnetic subband (or the intrinsic LL width) is set to zero. Figure 8 shows the dependence of $N_c/N_\phi^{1-1/(2\nu)}$ on system size for $\phi = 1/3, 1/7, 1/10$, and in the continuum model. The ratio is expected to be a horizontal line if ν is properly chosen and if there is no need for irrelevant length scale corrections. We compare the assumptions of $\nu = 2.48$ (supported by the current study) and 2.58 (supported

by a study of the lattice model without subband projection³⁰). Under the assumption of $\nu = 2.48$ as shown in Fig. 8(a), the ratio is essentially a constant for $\phi = 1/3$ and the continuum model for almost two orders of magnitude in N_ϕ . For $\phi = 1/7$ and $1/10$, the ratio stays convincingly as a constant up to the

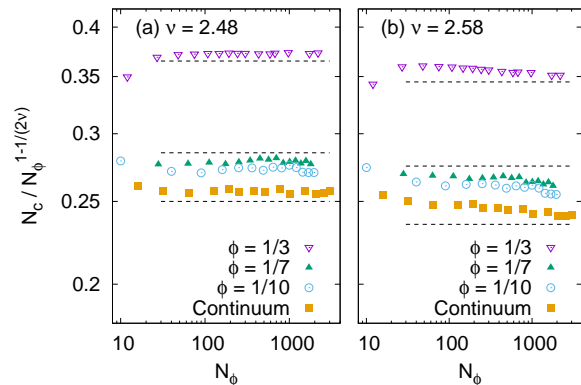


FIG. 8. System-size dependence of $N_c/N_\phi^{1-1/(2\nu)}$ for $\phi = 1/3, 1/7, 1/10$, and the continuum model under assumption of (a) $\nu = 2.48$ and (b) $\nu = 2.58$ for the localization length exponent ν . Horizontal dashed lines are guides to the eye only.

largest systems we can access using Chern number calculation with meaningful sample average. The relative uncertainties are about twice larger than the $\phi = 1/3$ case. The difference between the four cases lies in the finite-size deviation of the data. For $\phi = 1/3$, the ratio lies below the larger-system value for $L = 6$, or $N_\phi = 12$. For other cases of the lattice model and for the continuum model, the ratio for the smallest systems (not shown here for $\phi = 1/7$) lies above the corresponding larger-system value. The finite-size artifacts, however, do not affect the universality of the localization length exponent in these cases, according to Fig. 8(a). On the other hand, Fig. 8(b) tests the power-law scaling under the assumption $\nu = 2.58$. In sharp contrast to the results under $\nu = 2.48$, the larger exponent leads to clearly identifiable downward trend of the system-size dependence, regardless of the direction of the deviations in small systems. In fact, the best power-law fits without any corrections yield $\nu = 2.50 \pm 0.01$ for $\phi = 1/7$ ($N_\phi \geq 28$) and $\nu = 2.50 \pm 0.02$ for $\phi = 1/10$ ($N_\phi \geq 40$), both consistent with $\nu = 2.48 \pm 0.02$ within error bars.

Based on the comparison, we conclude that, at least in the projected lattice model, the power-law scaling with $\nu = 2.48$ describes the total number of conducting states well *without any need of corrections and regardless of the value of ϕ* . This seems to be the most natural conclusion, given that the same value is also supported by the continuum model, which can be regarded as the limit of vanishing ϕ . Unless extremely slowly developing corrections exist, the Chern number calculations of the projected lattice model and the continuum model do not support $\nu = 2.58$ or any value close.

¹ K. v. Klitzing, G. Dorda, and M. Pepper, Phys. Rev. Lett. **45**, 494 (1980).

² J. T. Chalker and P. D. Coddington, J. Phys. C **21**, 2665 (1988).

- ³ B. Huckestein and B. Kramer, Phys. Rev. Lett **64**, 1437 (1990).
- ⁴ Y. Huo and R. N. Bhatt, Phys. Rev. Lett. **68**, 1375 (1992).
- ⁵ D.-H. Lee, Z. Wang and S. Kivelson, Phys. Rev. Lett. **70**, 4130 (1993).
- ⁶ B. Huckestein, Rev. Mod. Phys. **67**, 357 (1995).
- ⁷ B. Kramer, T. Ohtsuki, and S. Kettemann, Phys. Rep. **417**, 211 (2005).
- ⁸ F. Evers and A. D. Mirlin, Rev. Mod. Phys. **80**, 1355 (2008).
- ⁹ W. Li, G. A. Csáthy, D. C. Tsui, L. N. Pfeiffer, and K. W. West, Phys. Rev. Lett. **94**, 206807 (2005).
- ¹⁰ W. Li, C. L. Vicente, J. S. Xia, W. Pan, D. C. Tsui, L. N. Pfeiffer, and K. W. West, Phys. Rev. Lett. **102**, 216801 (2009).
- ¹¹ K. Slevin and T. Ohtsuki, Phys. Rev. B **80**, 041304 (2009).
- ¹² H. Obuse, A. R. Subramaniam, A. Furusaki, I. A. Gruzberg, and A. W. W. Ludwig, Phys. Rev. B **82**, 035309 (2010).
- ¹³ M. Amado, A.V. Malyshev, A. Sedrakyan, and F. Domínguez-Adame, Phys. Rev. Lett. **107**, 066402 (2011).
- ¹⁴ J. P. Dahlhaus, J. M. Edge, J. Tworzydło, and C. W. J. Beenakker, Phys. Rev. B **84**, 115133 (2011).
- ¹⁵ I. C. Fulga, F. Hassler, A. R. Akhmerov, and C. W. J. Beenakker, Phys. Rev. B **84**, 245447 (2011).
- ¹⁶ K. Slevin and T. Ohtsuki, Int. J. Mod. Phys. Conf. Ser. **11**, 60 (2012).
- ¹⁷ H. Obuse, I. A. Gruzberg, and F. Evers, Phys. Rev. Lett. **109**, 206804 (2012).
- ¹⁸ I. A. Gruzberg, A. Klümper, W. Nuding, and A. Sedrakyan, Phys. Rev. B **95**, 125414 (2017).
- ¹⁹ R. Bondesan, D. Wieczorek, and M.R. Zirnbauer, Nucl Phys B **918**, 52 (2017).
- ²⁰ B. Huckestein, Europhys. Lett. **20**, 451 (1992).
- ²¹ B. Huckestein, Phys. Rev. Lett **72**, 1080 (1994).
- ²² K. Yang and R. N. Bhatt, Phys. Rev. Lett. **76**, 1316 (1996).
- ²³ R. N. Bhatt and X. Wan, Pramana J. Phys. **58**, 271 (2002).
- ²⁴ X. Wan, Ph.D. thesis, Princeton University (2000).
- ²⁵ D. J. Thouless, M. Kohmoto, M. P. Nightingale, and M. den Nijs, Phys. Rev. Lett. **49**, 405 (1982).
- ²⁶ Q. Niu, D. J. Thouless, and Y.-S. Wu, Phys. Rev. B **31**, 3372 (1985).
- ²⁷ T. Fukui, Y. Hatsugai, and H. Suzuki, J. Phys. Soc. Jpn. **74**, 1674 (2005).
- ²⁸ D. P. Arovas, R. N. Bhatt, F. D. M. Haldane, P. B. Littlewood, and R. Rammal, Phys. Rev. Lett. **60**, 619 (1988).
- ²⁹ W. H. Press, W. T. Vetterling, S. A. Teukolsky, and B. P. Flannery, *Numerical Recipes in C++: The Art of Scientific Computing*, 2nd ed. (Cambridge University Press, New York, NY, USA, 2002).
- ³⁰ M. Puschmann, P. Cain, M. Schreiber, and T. Vojta, arXiv:1805.09958.
- ³¹ M. R. Zirnbauer, arXiv:1805.12555.